iScience, Volume *24*

Supplemental Information

Cryo-EM structure of human mitochondrial HSPD1

David P. Klebl, Matthew C. Feasey, Emma L. Hesketh, Neil A. Ranson, Heiko Wurdak, Frank Sobott, Robin S. Bon, and Stephen P. Muench

Supplementary Figures

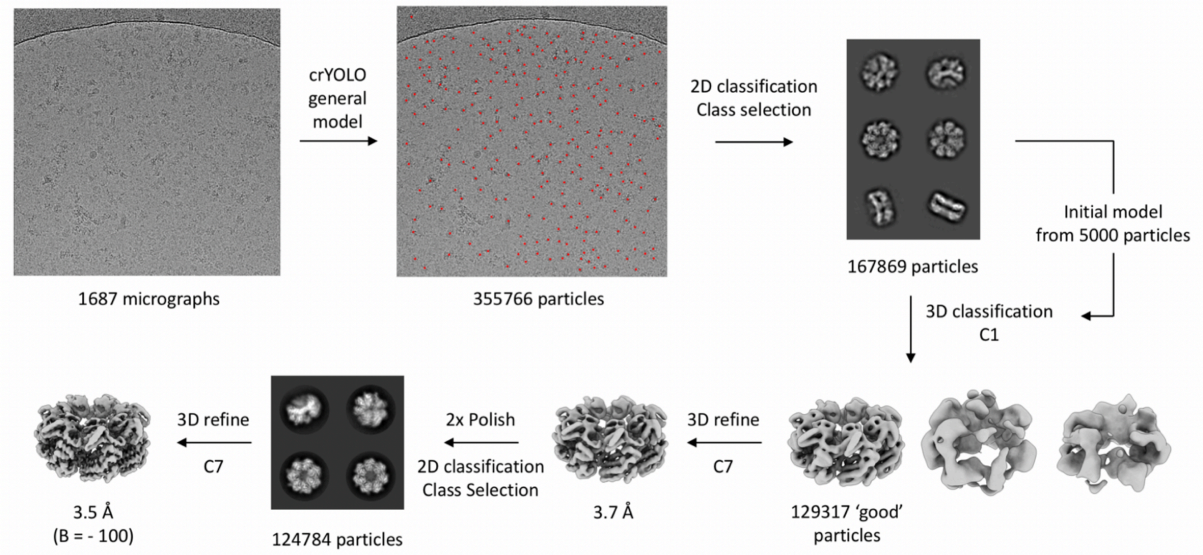

***Figure S1**. Summary of the data processing pipeline, Related to Table 1.* After motion correction and Ctf estimation, particles were picked using the general model in crYOLO. 2D classification yielded 167869 particles, which were subjected to 3D classification. 129317 particles were taken forward to refinement with C7 symmetry and Bayesian polishing. After polishing, 2D classification was used to select the final 124784 particles which were refined with C7 symmetry and filtered by local resolution using a B-factor of -100.

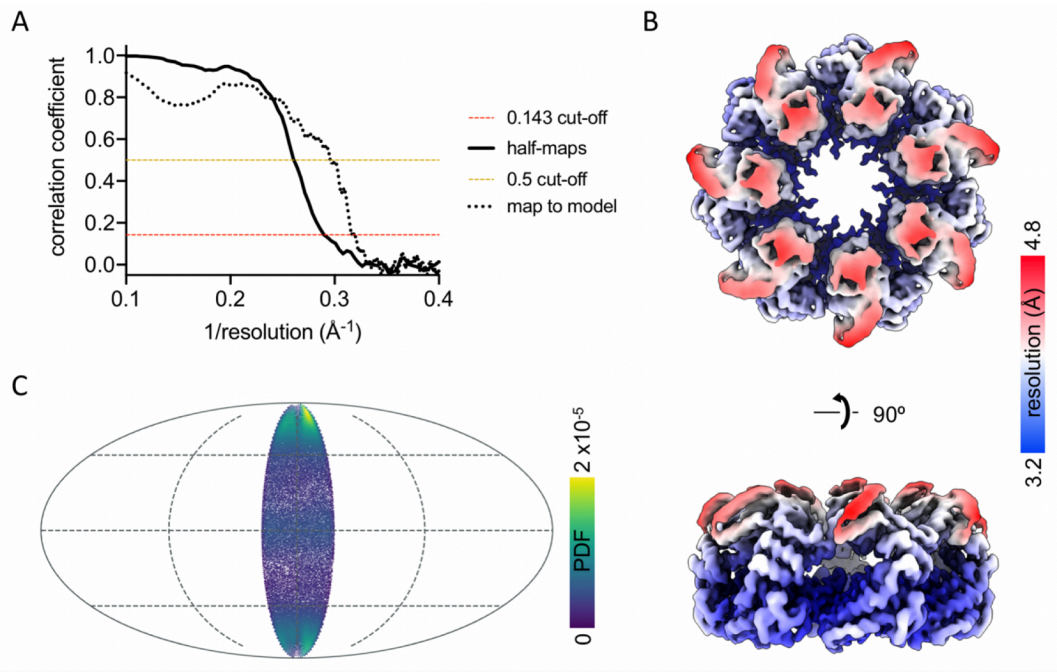

***Figure S2**. FSC curves, local resolution estimation and orientation distribution for HSPD1, Related to Figure 2.* (A) FSC curve for the final HSPD1 single ring reconstruction. Shown are the cut-off at 0.143 (red dashed line), the cut-off at 0.5 (yellow dashed line), correlation

between masked half-maps (black solid line) and correlation between map and model (black dotted line). (B) Local resolution in the HSPD1 single ring reconstruction. (C) Orientation distribution of the HSPD1 single ring particles, shown in Mollweide projection. PDF stands for probability density function, an estimate of the probability of finding a particle in any particular orientation.

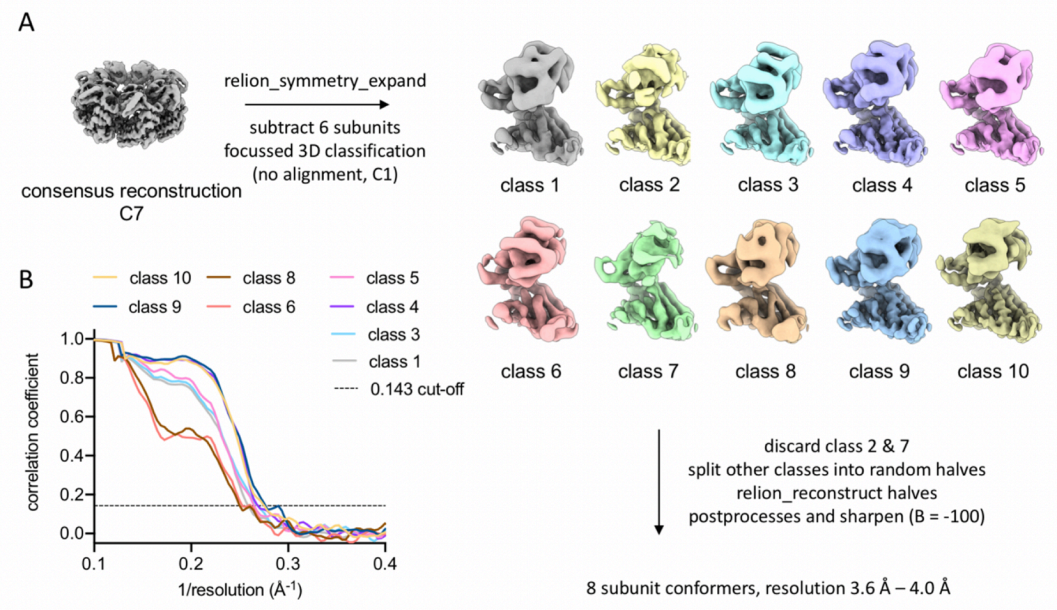

Figure S3*. Symmetry expansion of the single ring, Related to Figure 3.* (A) Starting point was the consensus reconstruction. The dataset was expanded, 6 of the 7 subunits subtracted and the subtracted particles classified without alignment. Of the 10 classes, 8 were taken forward to reconstruction and postprocessing, resulting in 8 subunit reconstructions at resolutions from 3.6 to 4.0 Å (FSC=0.143). FSC curves for these 8 reconstructions are shown in (B).

Transparent Methods

METHOD DETAILS

Protein expression and purification

An expression plasmid for mature HSPD1 (pMCSG7, containing cDNA for HSPD1, RefSeq NM_002156.4) was kindly provided by Dr Hao Shao and Dr Jason Gestwicki (University of California San Francisco, USA). Expression and purification of HSPD1 were based on a previously described protocol (Viitanen et al., 1998), also described in Klebl et al. 2020. Transformation of competent *E. coli* BL21 DE3 with the plasmid was carried out using the heat shock method (Hanahan 1983). Transformed cells were grown in 20 mL overnight cultures

(TB medium supplemented with 100 µg/mL ampicillin) for ~ 16 h at 37 °C. One litre of TB medium was then inoculated with 10 mL overnight culture and incubated at 37 °C under 200 rpm. When optical density at 600 nm reached 0.8, 250 µM IPTG (final concentration) was added to induce expression of HSPD1. Four hours after induction, the bacterial cells were harvested by centrifugation (10 min, 4000 rpm) and, until further usage, stored at -80 °C.

All purification steps prior to complex reconstitution were done at 4 °C or on ice. All volumes are given per 1 L of culture medium unless stated otherwise. Cell pellets were thawed on ice and resuspended in 20 mL lysis buffer (50 mM Tris, 500 mM NaCl, 10 mM imidazole pH 8), containing 1 mM PMSF and protease inhibitor cocktail (set V, Calbiochem). After further resuspending the cells in a dounce homogeniser, cell lysis was performed using sonication (10 min total, 35% amplitude, 30 sec on/off intervals). The lysate was cleared by centrifugation (30 min, 17,000 rpm) and the supernatant was applied to 3.5 mL Ni-NTA resin (equilibrated in lysis buffer). After washing the resin with 2x 100 mL lysis buffer and 100 mL of 50 mM Tris, 300 mM NaCl, 50 mM imidazole (pH 8), the protein was eluted with 10 mL of 50 mM Tris, 300 mM NaCl, 300 mM imidazole (pH 8). TEV protease (1.6 mg) and DTT (1 mM final concentration) were added and the solution was incubated for 4 h at RT. The cleaved protein was dialysed overnight into 50 mM Tris, 150 mM NaCl pH 7.5 (2 L) using 10 kDa molecular weight cutoff (MWCO) SnakeSkin dialysis tubing (ThermoFisher Scientific). The dialysis product was incubated with 1.5 mL Ni-NTA resin (pre-equilibrated in lysis buffer) for 1 h. The flowthrough was concentrated to 20 – 30 mg/mL in a spin concentrator (Vivaspin, Sartorius, 10 kDa MWCO) after adding 10% (v/v) glycerol. This procedure yielded about 1 - 2 mL at ~ 20 mg/mL per 1 L culture. Four millilitres concentrated, monomeric HSPD1 were mixed with 100 µL KCl (1 M), 100 µL $Mg(OAc)_2$ (1 M) and 400 µL Mg-ATP (50 mM, pH 7) and incubated for 90 min at 30 °C for reconstitution into oligomers. After centrifugation at 13,000 rpm for 10 min at RT, the supernatant was loaded onto a HiLoad 16/600 Superdex 200 gel filtration column (GE Healthcare) in 50 mM Tris, 300 mM NaCl, 10 mM $MgCl_2$ (pH 7.7).

Oligomeric and monomeric fractions were collected, pooled and concentrated to 10-25 mg/mL using spin concentrator (Vivaspin, Sartorius, 10 kDa MWCO). Concentrated protein was supplemented with 5% (v/v) glycerol, flash-frozen in liquid N_2 and stored at -80 °C. Protein concentration was measured using absorbance at 280 nm (ε_{280} = 14,440 $mol^{-1}cm^{-1}$, MW = 58.2 kDa). The purity was judged by SDS-PAGE, using Invitrogen™ Bolt™ 4-12% Bis-Tris Plus gels (ThermoFisher Scientific) according to the manufacturer's instructions.

Negative stain EM

For negative stain EM, in-house carbon coated 300 mesh Cu grids were used. Typically, grids were glow discharged in a Pelco easiGlow™ (Ted Pella) at 0.39 mbar, 12 mA for 30 s and used within 30 min. Three microliters of sample were applied to the grid, followed by incubation for 30 s, 2 washes with H_2O and application of 1 % uranyl acetate in two steps (1 min each). Grids were imaged using a FEI Tecnai T12 or a FEI Tecnai F20 microscope. Particle picking and 2D classification were done using crYOLO and RELION 3 (Wagner et al., 2019, Zivanov et al., 2018). Apo HSPD1 was used at 0.02-0.03 mg/mL in gel filtration buffer for negative stain EM.

Native mass spectrometry

For native mass spectrometry, HSPD1 was exchanged into 500 mM ammonium acetate using two consecutive Zeba spin desalting columns (Thermo Scientific) according to the manufacturer's instructions. The protein was diluted to a final concentration of ~ 0.5 mg/mL. Nano-electrospray capillaries were prepared in-house, using a P-97 micropipette puller (Sutter Instrument Co.) and coated with palladium/gold in a Polaron SC7620 sputter coater (Quorum Technologies). Native mass spectra were acquired on an Orbitrap Q Exactive Plus UHMR (Thermo Scientific) operated in positive ion mode. Instrument settings were: 1.5 kV capillary voltage, 20 V in source trapping and HCD off. The AGC target was set to 1e6 with a maximum inject time of 300 ms. The trapping gas pressure (ratio) was 7, resolution 12500 and the mass range was 2000 – 20000 m/z. Spectra were analysed using UniDec (Marty et al., 2015). The experimental error was estimated, for each charge state distribution, by multiplying the half width at half maximum of the most intense peak with the assigned charge.

Cryo-EM grid preparation

For cryo-EM grid preparation, Quantifoil R 1.2/1.3 300 mesh Cu grids were glow-discharged in a Cressington 208 carbon coater (with glow-discharge unit) at 10 mA and 0.1 mbar air pressure for 30 s. Grids were used within 30 min after the glow-discharge treatment. For cryo-EM, oligomeric HSPD1 was used at 2.3 mg/mL in 25 mM Tris, 150 mM NaCl, 5 mM $MgCl_2$, 1 mM DTT (pH 7.7). Grids were prepared on a Thermo/FEI Vitrobot mark IV, the relative humidity was ≥ 90% and temperature 20 °C. Liquid ethane was used as the cryogen. The blot force was 6 and blot time was 6 s. When grids were prepared with 50 mM Tris, 300 mM NaCl, 10 mM $MgCl_2$ (pH 7.7) buffer, they contained a small fraction (< 10 %) of inverted double ring particles.

Cryo-EM data collection and processing

Cryo-EM screening and data collection were done using a Thermo/FEI Titan Krios microscope equipped with a Falcon III direct electron detector operated in counting mode at the Astbury BioStructure Laboratory in Leeds. The main data acquisition parameters are given in Table 1 and an overview of the processing strategy is given in Figure S1. All processing was done using RELION 3, unless mentioned otherwise (Zivanov et al., 2018). Briefly, 1687 micrographs were collected. After correcting for beam-induced motion with MotionCor2 (Zheng et al. 2017) and Ctf-estimation using gctf (Zhang 2016), particles were picked using the general model in crYOLO (Wagner et al., 2019). One round of 2 D classification and one round of 3D classification gave a selection of 129317 'good' particles. The resolution (3.7 Å pre-polishing) was improved by 2 rounds of Bayesian polishing and an additional round of 2D classification to 3.5 Å. The final map was obtained by local-resolution filtering in relion using a sharpening B-factor of -100 (Figure S2).

The final particle set was then symmetry-expanded using relion_symmetry_expand. Density for six of the seven subunits was subtracted and focussed classification without image alignment was used to split the dataset into 10 classes. Visual inspection of the maps showed clear density for helices H and I in 8 classes, which were taken forward (Figure S3). For each of these classes, particles were split into random halves, each half reconstructed using relion_reconstruct and postprocessed (with a sharpening B-factor of -100).

Model building

An atomic model for the HSPD1 single ring was built and refined into the cryo-EM density using Coot, Isolde and Phenix (Emsley et al. 2010, Croll 2018, Liebschner et al. 2019). As starting models, the HSPD1-HSPE1 football crystal structure (PDB: 4pj1) and apo GroEL (PDB: 1xck) were used. Parts of these models were rigid-body docked into the EM density, mutated, and manually adjusted in Coot. The model was then iteratively adjusted and refined in Coot and Phenix. Small adjustments were also made using Isolde. Density was weak or not present for the C-terminus (residues 525-547), probably because these residues are highly flexible. Consequently, they were not modelled. The final model was validated using Molprobity (Chen et al. 2010). Atomic models for reconstructions from symmetry expansion were generated by docking the consensus model into the density and flexible fitting using adaptive distance restraints in Isolde. Atomic models and EM density were visualized using Chimera and ChimeraX (Pettersen et al. 2004, Goddard et al. 2018).

QUANTITATION AND STATISTICAL ANALYSIS

CryoEM data collection and processing were performed as described in single particle data collection and processing sections of the Methods Details using RELION3, MotionCor2, GCTF and crYOLO as detailed in the Key Resources Table.

References:

Chen, Vincent B., et al. "MolProbity: all-atom structure validation for macromolecular crystallography." Acta Crystallographica Section D: Biological Crystallography 66.1 (2010): 12-21.

Croll, Tristan Ian. "ISOLDE: a physically realistic environment for model building into low-resolution electron-density maps." Acta Crystallographica Section D: Structural Biology 74.6 (2018): 519-530.

Emsley, Paul, et al. "Features and development of Coot." Acta Crystallographica Section D: Biological Crystallography 66.4 (2010): 486-501.

Goddard, Thomas D., et al. "UCSF ChimeraX: Meeting modern challenges in visualization and analysis." Protein Science 27.1 (2018): 14-25.

Hanahan, Douglas. "Studies on transformation of Escherichia coli with plasmids." *Journal of molecular biology* 166.4 (1983): 557-580.

Liebschner, Dorothee, et al. "Macromolecular structure determination using X-rays, neutrons and electrons: recent developments in Phenix." Acta Crystallographica Section D: Structural Biology 75.10 (2019): 861-877.

Marty, Michael T., et al. "Bayesian deconvolution of mass and ion mobility spectra: from binary interactions to polydisperse ensembles." Analytical chemistry 87.8 (2015): 4370-4376.

Pettersen, Eric F., et al. "UCSF Chimera—a visualization system for exploratory research and analysis." Journal of computational chemistry 25.13 (2004): 1605-1612.

Wagner, Thorsten, et al. "SPHIRE-crYOLO is a fast and accurate fully automated particle picker for cryo-EM." Communications biology 2.1 (2019): 1-13.

Zhang, Kai. "Gctf: Real-time CTF determination and correction." Journal of structural biology 193.1 (2016): 1-12.

Zheng, Shawn Q., et al. "MotionCor2: anisotropic correction of beam-induced motion for improved cryo-electron microscopy." Nature methods 14.4 (2017): 331-332.

Zivanov, Jasenko, et al. "New tools for automated high-resolution cryo-EM structure determination in RELION-3." Elife 7 (2018): e42166.